

Multiple Tuning of Birdcage Resonators

Smain Amari, Aziz Müfit Uluğ, Jens Bornemann, Peter C. M. van Zijl, Peter B. Barker

A theoretical framework is presented for designing birdcage resonators for MRI and MR spectroscopy. The analogy between the birdcage problem and the phonon problem in solid-state physics is used to achieve multiple tuning. Allowing that the capacitances in the columns of the cage assume unequal values, it is possible to achieve multiple tuning and simultaneously preserve the sinusoidal current distribution necessary to set a homogeneous magnetic field. Given the physical dimensions of the columns and branches of the cage as well as the desired resonant frequencies, the corresponding values of the capacitances can be calculated exactly. Closed-form expressions for the capacitances are given in terms of the mutual inductances and the desired resonant frequencies. A detailed analysis for a symmetrical low-pass birdcage is presented. The expressions for the resonant frequencies reduce to those given by other authors when only nearest-neighbor mutual inductances are included.

Key words: double-tuned; birdcage; coil; resonator.

INTRODUCTION

Many experiments for *in vivo* MR spectroscopy require double-tuned or multituned RF coils. For example, double-tuned resonators are preferred when studying uptake and metabolism of ^{13}C -glucose by proton-detected ^{13}C NMR (1–7) or proton-decoupled ^{13}C NMR (8). In addition, recent studies have shown the importance of applying proton decoupling when using phosphorus NMR, leading to increased interest in double-tuned coil design (9, 10).

The original NMR birdcage resonator, introduced by Hayes *et al.* (11), was single-tuned and exhibited an improvement in both the field homogeneity and the signal-to-noise ratio (SNR) over the saddle coil as well as cosine coil (12). The introduction of quadrature drive of the volume coil resulted in a reduction of power requirement by a factor of 2 and an increase of SNR by a factor of $\sqrt{2}$ compared with linear coils (11, 13). A theoretical investigation of birdcage resonators was presented by Tropp (14), including the effect of perturbations in the capacitances. Pascone *et al.* (15) used the concept of effective inductance, which includes all mutual inductances, to describe the frequency response of high- and

low-pass resonators. Foo *et al.* (16) analyzed the effect of the body as well as the shield, by solving Maxwell's equation in a cylindrically symmetrical structure, whereas Harpen (17, 18) described the equivalent circuits for resonators with a large number of columns as well as the behavior near self-resonance.

The analysis and design of multituned birdcage resonators has also been investigated in recent years. Rath (19) introduced a double-tuned design based on band-stop and band-pass filters, which can only be used at one of its two possible frequencies at a given time. Joseph and Lu (20) analyzed nonuniform distribution of capacitances in the columns of birdcage resonators and showed that a judicious choice of such a distribution could lead to a double-tuned resonator, as long as the two frequencies are not too different. Recently, resonators using more than two rings were reported by Boesch *et al.* (21) and Tropp *et al.* (22). Coaxial cavity-type volume coils were also implemented (23–24). Double-tuned saddle resonators were also reported (see Ref. 25 and references cited within). In general, double-tuned resonators tend to be difficult to build and may be difficult to tune to the desired operating frequencies.

Here, we describe a novel and simple theoretical approach to analyze, design, and tune a birdcage resonator to one or multiple frequencies. A symmetrical low-pass birdcage, including all mutual inductances of the columns as well as the ring segments, is analyzed in the next section, Modes of Symmetrical Birdcage Coil. Expressions for the resonant frequencies in terms of self- and mutual inductances and capacitances are also given. In the section entitled Double Tuning within Nearest-Neighbor Approximation, the solution to the phonon problem in solid-state physics is used to show how a simple and well-defined distribution of capacitances in the columns leads to a double-tuned resonator. Given the physical dimensions of the resonators, simple expressions for the two capacitances required for double tuning to two arbitrary frequencies are given. The next section, Beyond the Nearest-Neighbor Approximation, discusses the effect of the mutual inductances on the capacitance values, and is followed by a section on the problem of multiple tuning. Finally, under Results, numerical results obtained from the present method are presented and compared with experimental values.

MRM 37:243–251 (1997)

From the Centre for Advanced Materials and Related Technology, University of Victoria, Victoria, British Columbia, Canada (S.A., J.B.); Department of Radiology, NMR Research Division, Johns Hopkins University School of Medicine, Baltimore, Maryland (A.M.U., P.C.M.vZ.); and Department of Neurology, Henry Ford Hospital, Detroit, Michigan (P.B.B.).

Address correspondence to: Aziz M. Uluğ, Ph.D., Department of Radiology, NMR Research Division, Johns Hopkins University School of Medicine, 217 Traylor Building, 720 Rutland Avenue, Baltimore, MD 21205-2195.

Received March 7, 1996; revised May 24, 1996; accepted July 23, 1996.

This work is supported in part by the Whitaker Foundation (PvZ) and by National Institutes of Health Grant NS 31490 (PvZ).

0740-3194/97 \$3.00

Copyright © 1997 by Williams & Wilkins

All rights of reproduction in any form reserved.

MODES OF SYMMETRICAL BIRDCAGE COIL

We first consider a symmetrical low-pass bird cage with N identical columns, as shown in Fig. 1, and assume perfectly conducting foil segments and equal capacitances in the columns. The analysis can then be extended to high-pass coils with capacitances on the rings. The foil segments in the birdcage are modeled as inductances, L for the columns and l for the portions of the rings as shown in Fig. 2. In order not to overcrowd the equations,

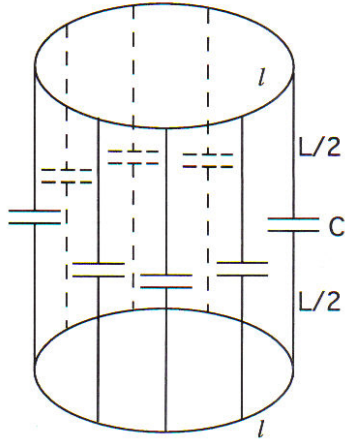


FIG. 1. An eight-column low-pass birdcage resonator: l is the self-inductance of the ring portion between two adjacent columns, L is the self-inductance of a single column, and C is the capacitor placed on each column.

the mutual coupling between the top and bottom rings are neglected in the main discussion. Appendix A gives the modified equations when all mutual inductances are included. The mutual inductance between two consecutive columns, nearest neighbors, will be denoted by $M = M_1$; M_2 denotes the mutual inductance between the second nearest neighbors; in general, M_i denotes the i th nearest neighbors' mutual inductance. We also neglect the mutual inductance between consecutive ring segments. Appendix A gives the corrections relevant to these terms.

A resonant mode, with unknown angular frequency ω , is excited in the structure. To proceed with the analysis, a mesh current I_n is assumed to flow clockwise in the closed path consisting of columns n and $n + 1$ and the ring segments connecting them. The actual current in leg n is then given by $I_n - I_{n-1}$, whereas that flowing in the ring segment is simply I_n (Fig. 2).

The application of Kirchoff's law to mesh n leads to the following equation:

$$\begin{aligned} & \left[(2L + 2l - 2M)\omega^2 - \frac{2}{C} \right] I_n \\ & - \left[(L - 2M + M_2)\omega^2 - \frac{1}{C} \right] [I_{n-1} + I_{n+1}] \\ & - [(M - 2M_2 + M_3)\omega^2][I_{n+2} + I_{n-2}] - \dots = 0 \end{aligned} \quad [1]$$

where C is the common value of the capacitances. The sum includes all the mutual inductances between the columns; those of the ring segments are neglected as stated above. Equation [1] can be viewed as an eigenvalue problem for the frequency ω once the geometrical and physical characteristics of the cage are specified. A running solution to this equation can be found either by

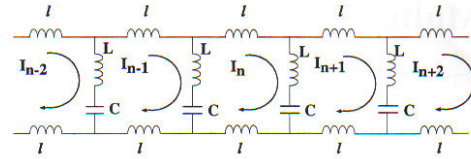


FIG. 2. Model of the resonator with mesh currents.

taking a discrete Fourier transform or simply by trying a solution of the form

$$I_n = Ae^{j(\omega t - (2\pi n/N))} \quad [2]$$

where J is the "wavenumber." Because of the periodicity of the system, i.e., $I_n + N = I_n$, J should satisfy the equation

$$e^{j(2\pi J)} = 1 \quad [3]$$

which implies that J should assume integer values. It is convenient to limit the range of J values to what is known in solid-state physics as the first Brillouin zone (26; 27, p. 100; 28, p. 105). In this particular case, this zone limits the values of J to

$$-\frac{N}{2} < J \leq \frac{N}{2} \quad [4]$$

It is always possible to replace a value of J that lies outside the first zone by one inside it by adding an appropriate multiple of the period N . Details can be found in several textbooks on solid-state physics (26-29).

Each value of J corresponds to one or more resonant modes whose frequencies are simply obtained by substituting Eq. [2] in Eq. [1] and noting that the terms of the form $I_{n+i} + I_{n-i}$ are related to I_n by

$$I_{n-i} + I_{n+i} = 2I_n \cos\left(\frac{2\pi i J}{N}\right) \quad [5]$$

Carrying out the algebra and rearranging Eqs. [1] to [3], we get the resonant frequency of mode J :

$$\omega_j^2 = a_0 \frac{\left(1 - \cos\left(\frac{2\pi J}{N}\right)\right)}{1 - \sum_{n=1}^{n=P} \left(\frac{a_n}{a_0}\right) \cos\left(\frac{2\pi J n}{N}\right)} \quad [6]$$

The denominator includes P terms, where $P = \{N/2\}$ if N is even and $\{N-1/2\}$ if N is odd. Note also that we use the index J to denote a particular mode to conform to the notations used by Tropp (14). The constants a_i are expressed in terms of the parameters of the birdcage

$$a_0 = \frac{1}{C(L + l - M)} \quad [7a]$$

$$a_1 = \frac{1}{C(L - 2M + M_2)} \quad [7b]$$

$$a_i = \frac{1}{C(M_{i-1} - 2M_i + M_{i+1})}, \quad i = 2, 3, \dots, p \quad [7c]$$

Note that our result (Eq. [6]) reduces to Tropp's (14), if the terms in a_i for $i \geq 2$ are neglected.

Among all the resulting modes, only the mode $J = 1$ has the sinusoidal current distribution required to establish a uniform magnetic field inside the cage (30). The other modes do not have this important homogeneity property and are consequently of little interest.

From the present analysis, it follows that the symmetrical birdcage does not allow for homogeneous multiple tuning, because there is only one frequency for the homogeneous mode $J = 1$. A possible approach to double tuning, which has been investigated in detail by Joseph and Lu (20), consists of introducing a perturbation that eliminates the degeneracy of the homogeneous mode, thereby achieving double tuning. This approach is expected to work well as long as the two resonant frequencies are not too different such that perturbation theory can be fruitfully used to determine the properties of the two perturbed modes. When the two frequencies become widely separated, the analysis fails and the homogeneity in the magnetic field becomes unacceptable. Furthermore, the approach cannot be used to tune the resonator to more than two frequencies. It is also possible to use more than two rings and tune each "subcage" to different frequencies with appropriate consideration of the mutual interactions between the subcages as presented by Pascone *et al.* (15). In the next section, we show how double tuning can be achieved by a judicious, yet systematic, choice of the capacitances without sacrificing the homogeneity of the magnetic field, provided a large enough number of columns are used. For ease of construction, we demonstrate the principle by building a coil with eight columns.

DOUBLE TUNING WITHIN NEAREST-NEIGHBOR APPROXIMATION

Tuning the birdcage to two arbitrary frequencies can be achieved if the period of the structure is enlarged to include two original meshes. Taking the capacitances in the columns of the cage in Fig. 1 such that $C_0 = C_2 = C_4 = \dots = C_{\text{even}}$ and $C_1 = C_3 = C_5 = \dots = C_{\text{odd}}$, while keeping the locations and dimensions of the wires unchanged, doubles the period of the structure. Other choices, such as alternately changing the locations of the wires while keeping all other parameters fixed, are also possible. In this study, we consider only the former arrangement. The analysis of the resulting asymmetrical birdcage is similar to the symmetrical one except for the fact that the n th and $(n + 1)$ th meshes should be treated differently. The problem is analogous to the propagation of elastic waves (phonons) in a periodic chain of atoms whose Bravais lattice contains a basis (26–29). In fact, the qualitative features of the modes of the present system are practically the same as those of a periodic linear chain containing two different masses, M and m , which are interacting through springs of identical stiffness. For the sake of completeness, and for readers not familiar with the

theory of lattice vibrations, we present a detailed analysis of the asymmetrical birdcage. Also, in order not to bury the main idea in the notations, we assume that only nearest neighbors interact, i.e., $M_i = 0$, $i \geq 2$. This constraint will be relaxed later.

The currents in mesh n are denoted by X_n , that in mesh $n + 1$ by Y_n , and so on (Fig. 3). The equations governing X_n and Y_n follow from applying Kirchoff's law:

$$\begin{aligned} & \left[(2L + 2l - 2M)\omega^2 - \left(\frac{1}{C_{\text{odd}}} + \frac{1}{C_{\text{even}}} \right) \right] X_n \\ & - M\omega^2 [X_{n-1} + X_{n+1}] - \left[(L - 2M)\omega^2 - \frac{1}{C_{\text{even}}} \right] Y_n \\ & - \left[(L - 2M)\omega^2 - \frac{1}{C_{\text{odd}}} \right] Y_{n-1} = 0 \end{aligned} \quad [8]$$

$$\begin{aligned} & \left[(2L + 2l - 2M)\omega^2 - \left(\frac{1}{C_{\text{odd}}} + \frac{1}{C_{\text{even}}} \right) \right] Y_n \\ & - M\omega^2 [Y_{n-1} + Y_{n+1}] - \left[(L - 2M)\omega^2 - \frac{1}{C_{\text{even}}} \right] X_n \\ & - \left[(L - 2M)\omega^2 - \frac{1}{C_{\text{odd}}} \right] X_{n+1} = 0 \end{aligned} \quad [9]$$

Separate running solutions of the following forms are used for X_n and Y_n :

$$X_n = A e^{i(n-1/2)2\pi n/K} \quad [10a]$$

$$Y_n = B e^{i(n-1/2)2\pi n/K} \quad [10b]$$

Here, A and B are the complex constants of proportionality. They carry the information about phase lag of the currents in adjacent columns through their imaginary components or through their phases. The information about the relative currents in adjacent columns is revealed in the magnitudes of A and B . The term K , instead of N , was purposely used to emphasize the fact that the period is now doubled because the capacitances are not all equal. This also means that the total number of columns must be even to be able to split them into two distinct groups. Therefore, K in Eq. [10] is equal to $N/2$. From the periodicity requirement, it follows that J can assume the values such that $-K/2 < J \leq K/2$. Using Eq. [10] in the equations of motion, Eqs. [8] and [9], a system of two linear equations with unknowns A and B , is obtained:

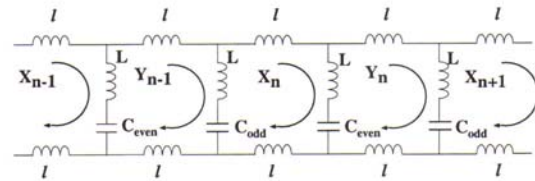


FIG. 3. Mesh currents with unequal capacitances for double tuning.

$$\left[\left(2L + 2l - 2M - 2M \cos \left(J \frac{2\pi}{K} \right) \right) \omega_j^2 - \left(\frac{1}{C_{\text{odd}}} + \frac{1}{C_{\text{even}}} \right) \right] A \quad [11a]$$

$$+ \left[\left(2M - L \right) \omega_j^2 + \frac{1}{C_{\text{even}}} + e^{j\beta(2\pi/K)} \left(2M - L \right) \omega_j^2 + \frac{1}{C_{\text{odd}}} \right] B = 0$$

$$\left[\left(2M - L \right) \omega_j^2 + \frac{1}{C_{\text{even}}} + e^{-j\beta(2\pi/K)} \left(2M - L \right) \omega_j^2 + \frac{1}{C_{\text{odd}}} \right] A \quad [11b]$$

$$+ \left[\left(2L + 2l - 2M - 2M \cos \left(J \frac{2\pi}{K} \right) \right) \omega_j^2 - \left(\frac{1}{C_{\text{odd}}} + \frac{1}{C_{\text{even}}} \right) \right] B = 0$$

Such a system admits a nontrivial solution only if its determinant vanishes. This last condition is satisfied for frequencies given by the following quadratic equation in the square of the frequency

$$a\omega_j^4 + b\omega_j^2 + c = 0 \quad [12]$$

where

$$a = a_1^2 - 2(L - 2M)^2 \left(1 + \cos \left(J \frac{2\pi}{K} \right) \right) \quad [13a]$$

$$b = -2 \left(\frac{1}{C_{\text{odd}}} + \frac{1}{C_{\text{even}}} \right) \left(2L + 2l - L \left(1 + \cos \left(J \frac{2\pi}{K} \right) \right) \right) \quad [13b]$$

$$c = \frac{2}{C_{\text{odd}} C_{\text{even}}} \left(1 - \cos \left(J \frac{2\pi}{K} \right) \right) \quad [13c]$$

$$a_1 = 2L + 2l - 2M \left(1 + \cos \left(J \frac{2\pi}{K} \right) \right) \quad [13d]$$

The resonant frequencies are the positive roots of Eq. [12] or

$$\omega_j^2 = \frac{-b \pm \sqrt{b^2 - 4ac}}{2a} \quad [14]$$

For each value of J , there are two modes, each of which degenerate, having different frequencies corresponding to the \pm sign in Eq. [14]. The degeneracy originates from the fact that $-J$ and J of Eq. [4] yield the same resonant frequency. There is also a gap in the frequencies that are supported by this structure, in the limit of large numbers of columns. This feature is also found in phonon spectra and in the energy-band theory of solids (26–29). In the limit of large numbers of columns in the birdcage, the resonant frequencies are continuously distributed in two branches. These two branches are named in analogy to their use in crystal vibrations theory, i.e., the optical and acoustic branches. The acoustic branch is characterized by the fact that the $J = 0$ has a frequency equal to zero, whereas the optical branch has the highest resonant frequency supported by the structure. The frequencies in the acoustic branch increase with the mode order J until they reach a maximum at $J = K/2$. On the contrary, the

frequencies in the optical branch decrease from the highest frequency at $J = 0$ to reach a minimum when $J = K/2$. At the boundary of the first Brillouin zone, $J = K/2$, the two branches are split by a gap whose magnitude increases with the difference $C_{\text{odd}} - C_{\text{even}}$. Figure 4 shows the qualitative features of the two branches that could be directly compared to those of the crystal vibrations found in Refs. 26 to 29.

The current distribution of the modes $J = 1$ follows immediately from Eq. [10]. Both have the sinusoidal distribution necessary for a homogeneous magnetic field inside the cage. There is, however, a phase difference between the currents in even-numbered and odd-numbered meshes. Once the desired resonant frequencies are known, Eqs. [12] to [14] can be used to determine the value of the capacitances C_{even} and C_{odd} ; the values of the mutual and self-inductances are known from the dimensions and the locations the wires. Within the nearest-neighbor-only approximation, C_{even} and C_{odd} are given by

$$C_{\text{odd,even}} = \frac{2}{S_r \pm \sqrt{S_r^2 - 4P_r}} \quad [15]$$

where

$$S_r = \frac{a}{2} \frac{\omega_1^2 + \omega_2^2}{2L + 2l - L \left(1 + \cos \left(\frac{2\pi}{K} \right) \right)} \quad [16a]$$

$$P_r = \frac{a}{2} \frac{\omega_1^2 \omega_2^2}{1 - \cos \left(\frac{2\pi}{K} \right)} \quad [16b]$$

The constant a is given by Eq. [13.a], and the frequencies ω_1 and ω_2 are the desired (known) frequencies of the two modes with the sinusoidal current distribution. Note that the two resonant frequencies are arbitrary and do not have to be close to each other for the present analysis to hold.

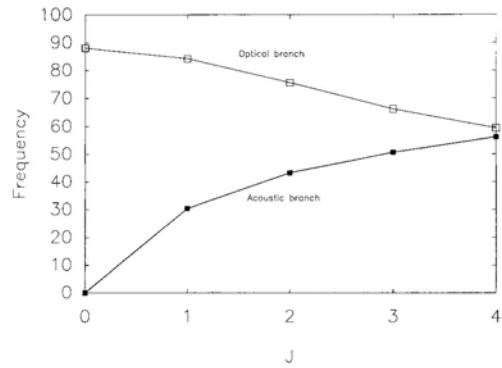


FIG. 4. The frequency dependence of the modes of optical and acoustic branch for a 16-column low-pass double-tuned resonator with $C_{\text{even}} = 0.9C_{\text{odd}}$. The duplicity of the modes for each value of J is evident.

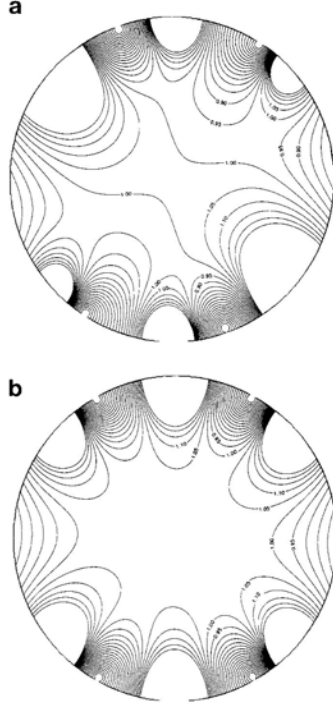


FIG. 5. Calculated field homogeneity of the eight-legged double-tuned birdcage coil: (a) optical mode (64 MHz), (b) acoustic mode (16 MHz).

Using Eqs. [15], [14], and [11], the ratio A/B is calculated. Then, utilizing Eq. [10] and the ratio A/B , the current in each column is computed. From these currents, the field map was calculated using the Biot-Savart law (Fig. 5).

BEYOND THE NEAREST-NEIGHBOR APPROXIMATION

In this section, we relax the nearest-neighbor-only approximation and investigate the problem of tuning the birdcage, including all mutual inductances of the columns. For clarity, the mutual inductances of the ring segments are still neglected here. Formulas given in Appendix B include all the mutual inductances and should, therefore, be used for the design and analysis of this type of resonator.

The inclusion of all the mutual inductances between the columns modifies Eqs. [8] and [9] to:

$$\begin{aligned} & \left[(2L + 2l)\omega^2 - \left(\frac{1}{C_{\text{odd}}} + \frac{1}{C_{\text{even}}} \right) \right] X_n \\ & - \left[L\omega^2 - \frac{1}{C_{\text{even}}} \right] Y_n - \left[L\omega^2 - \frac{1}{C_{\text{odd}}} \right] Y_{n-1} \end{aligned}$$

$$\begin{aligned} & + \sum_{i=0}^{K/2-1} M_{2i+1} [2Y_{n+i} + 2Y_{n-i-1} - X_{n-i-1} \\ & - X_{n-i} - X_{n+i} - X_{n+i+1}] \omega^2 \end{aligned} \quad [17]$$

$$\begin{aligned} & + \sum_{i=1}^{K/2} M_{2i} [2X_{n+i} + 2X_{n-i} - Y_{n+i} - Y_{n+i-1} \\ & - Y_{n-i} - Y_{n-i-1}] \omega^2 = 0 \end{aligned}$$

and

$$\begin{aligned} & \left[(2L + 2l)\omega^2 - \left(\frac{1}{C_{\text{odd}}} + \frac{1}{C_{\text{even}}} \right) \right] Y_n \\ & - \left[L\omega^2 - \frac{1}{C_{\text{even}}} \right] X_n - \left[L\omega^2 - \frac{1}{C_{\text{odd}}} \right] X_{n+1} \end{aligned}$$

$$\begin{aligned} & + \sum_{i=0}^{K/2-1} M_{2i+1} [2X_{n+i+1} + 2X_{n-i} - Y_{n-i} \\ & - Y_{n-i-1} - Y_{n+i+1} - Y_{n+i}] \omega^2 \end{aligned} \quad [18]$$

$$\begin{aligned} & + \sum_{i=1}^{K/2} M_{2i} [2Y_{n+i} + 2Y_{n-i} - X_{n+i} - X_{n-i} \\ & - X_{n+i+1} - X_{n-i+1}] \omega^2 = 0 \end{aligned}$$

As before, $K = N/2$, because the total number of columns is assumed to be even to achieve double tuning. For simplicity, it is also assumed that K is itself even or, equivalently, that N is a multiple of 4. Notice that Eqs. [17] and [18] reduce to Eqs. [8] and [9] if the mutual inductances beyond $M_i = M$ are neglected.

Running solutions of the form [10] are again used in Eqs. [17] and [18] and lead to two coupled linear equations in the constants A and B . The final result can be written as

$$\begin{aligned} a_{11}A + a_{12}B &= 0 \\ a_{21}A + a_{22}B &= 0 \end{aligned} \quad [19]$$

where

$$a_{11} = a_{22} = b_{11}\omega^2 - \left(\frac{1}{C_{\text{odd}}} + \frac{1}{C_{\text{even}}} \right) \quad [20a]$$

$$a_{12} = a_{21}^* = -b_{12}\omega^2 + \left(\frac{1}{C_{\text{even}}} + \frac{e^{j(2\pi/K)}}{C_{\text{odd}}} \right) \quad [20b]$$

$$\begin{aligned} b_{11} &= 2L + 2l - 2M \left(1 + \cos\left(\frac{2\pi}{K}\right) \right) \\ &+ \sum_{i=1}^{i=K/2} (2M_{2i} - 2M_{2i+1}) \cos\left(\frac{2\pi}{K} i\right) \end{aligned} \quad [21a]$$

$$\begin{aligned}
& - 2M_{2i+1} \cos\left(\frac{2\pi J}{K}(i+1)\right) \\
b_{12} = L - 2M + & \sum_{i=1}^{j=K/2} 2M_{2i} \cos\left(\frac{2\pi J}{K}i\right) (1 + e^{j(2\pi/K)}) \\
& - \sum_{i=1}^{i=K/2} 2M_{2i+1} [e^{j(2\pi/K)(i+1)} + e^{-j(2\pi/K)i}]
\end{aligned} \tag{21b}$$

The linear set of Eq. [19] admits a nontrivial solution only for frequencies ω for which the determinant of the system vanishes, $a_{11}a_{22} - a_{12}a_{21} = 0$. This last condition gives the resonant frequencies of the structure for the different values of J (resonant modes). Because we are interested in double tuning the birdcage to two known frequencies ω_1 and ω_2 , while having a sinusoidal current distribution, we only give the expressions of the capacitances C_{odd} and C_{even} , which achieve such tuning, namely

$$C_{\text{odd,even}} = \frac{2}{S_i \pm \sqrt{S_i^2 - 4P_i}} \tag{22}$$

The quantity S_i is related to the sum of the squares of the two resonant frequencies through

$$S_i = \frac{(b_{11}^2 - |b_{12}|^2)(\omega_1^2 + \omega_2^2)}{2b_{11} - b_{12} - b_{12}^*} \tag{23}$$

On the other hand, P_i is related to the product of the squares of the two resonant frequencies by

$$P_i = \frac{(b_{11}^2 - |b_{12}|^2)\omega_1^2\omega_2^2}{2\left(1 - \cos\left(\frac{2\pi}{K}\right)\right)} \tag{24}$$

In Eqs. [23] and [24], b_{11} and b_{12} are for $J = 1$. Notice that Eq. [23] reduces to Eq. [15] if the terms in $M_i > 1$ are neglected. Once the two resonant frequencies are known, the values of the capacitances are determined from Eq. [22]. The corresponding current distribution is obtained from Eq. [10], once the frequencies are known, and $J = 1$ for the sinusoidal modes. It is worth emphasizing that the current distributions for the different modes depend only on the fact that the structure is periodic. The values of the resonant frequencies and the strength of the magnetic field are determined by the physical properties of the system. In other words, two birdcages with identical periods have similar current distributions (they belong to the same symmetry group) but may have different resonant frequencies. For example, a low-pass birdcage has the same current profile as a high-pass birdcage with the same number of periods but different resonant frequencies. It is also possible to exploit this property of the symmetry group to achieve multiple tuning provided enough columns are used.

MULTIPLE TUNING

In this section, we briefly show how multiple tuning of a birdcage can be achieved. We again borrow from the results of the lattice vibration theory. It is well established that a periodic chain having p different atoms per unit cell (Bravais lattice) has p phonon branches, each in turn having N modes, where N is the number of periods in the chain (26, 28). For the birdcage problem, if there are enough columns to allow for a reasonably homogeneous magnetic field, it suffices to distribute the capacitances in the columns such that $C_0 = C_p = C_{2p}$, $C_1 = C_p + 1 = C_{2p+1}$, and so on while maintaining the original (symmetric) distribution of the wires to tune the structure to p different frequencies at the $J = 1$ mode. Such a birdcage exhibits p modes, which have the sinusoidal current distribution in p different frequencies. The determination of the values of the capacitances from the dimensions of the wires and their locations and the resonant frequencies may be numerically demanding but is otherwise straightforward.

RESULTS

We built a birdcage with eight columns of usable height $h = 19.1$ cm and diameter $D = 15.4$ cm, where the distance between consecutive columns is $s = 5.9$ cm. Copper foil of width $a = 1.3$ cm, and negligible thickness is used for the columns and the rings.

The self-inductance of one of the columns is given by an expression of Grover (Eq. [9] on p.35 in Ref. 31), which is also given in Ref. 15, namely

$$L = 2h \left[\ln\left(\frac{2h}{b}\right) + \frac{1}{2} \right] \tag{25}$$

where L is the inductance in nanohenries, h is the height in cm, and b is the width in centimeters of the rectangular strip. Similarly, the mutual inductance between two parallel segments of length h and separation d is given (Eq. [1] on p. 31 in Ref. 31) by

$$M = 2h \left[\ln\left(\frac{h}{d} + \sqrt{1 + \left(\frac{h}{d}\right)^2}\right) - \sqrt{1 + \left(\frac{d}{h}\right)^2} + \frac{d}{h} \right] \tag{26}$$

Here as well, distances are measured in centimeters and inductances in nanohenries. By assuming no skin effect and using the above expressions, we calculated the values of mutual inductances for our eight-legged birdcage and tabulated them in Table 1. In these calculations, axial filament approximation was used. The formulas used to calculate the mutual inductances between the ring segments are from Grover (Eqs. [52] and [53] on p. 56 in Ref. 31) and also in Ref. 15. The calculated resonant frequencies are shown in Fig. 6. The results obtained from Eq. [6], with only the mutual inductances between the birdcage columns included, are shown as solid lines. The results obtained from Eq. [A.2] in Appendix A, where the mutual inductances of the ring segments are all included, are shown as dotted lines. The percentage error on the frequency of the $J = 1$ mode varies from less than 2% for $C = 47$ pF to 22% for $C = 10$ pF.

Table 1
Calculated Self- and Mutual Inductances for the Eight-Legged Birdcage Resonator

$L = 0.148 \mu\text{H}$
$l = 0.0324 \mu\text{H}$
$M = M_1 = 0.0437 \mu\text{H}$
$M_2 = 0.0283 \mu\text{H}$
$M_3 = 0.0228 \mu\text{H}$
$M_4 = 0.0213 \mu\text{H}$
$m_0 = 0.00183 \mu\text{H}$
$m_{1B} = 0.00322 \mu\text{H}$
$m_{3B} = 0.00261 \mu\text{H}$
$m_{4B} = 0.00147 \mu\text{H}$
$m_{1T} = 0.00614 \mu\text{H}$
$m_{3T} = 0.00194 \mu\text{H}$
$m_{4T} = 0.00252 \mu\text{H}$

The discrepancy between the calculated and measured resonant frequencies is sensitive to the presence of a small capacitance in parallel with C . Indeed, an additional 2 pF in the gap (of width 0.13 mm) improves the agreement to 12% when $C = 10$ pF without appreciably affecting the results at larger values of C .

The same birdcage is now double tuned at 1.5 Tesla to the proton and carbon frequencies, 64 and 16 MHz, respectively. The values of the self- and mutual inductances are still those given in Table 1. The values of the capacitances necessary for double tuning, as calculated from Eq. [15] are listed in Table 2 along with their experimental values. The experimental values are the actual manufacturer-specified capacitance values. The capacitors we used are rated 1% accurate by the manufacturer (American Technical Ceramics, Huntington Station, NY). We used two capacitors in parallel on each leg so that the total capacitance is: $C_{\text{odd}} = 526$ pF ($526 = 470 + 56$) and $C_{\text{even}} = 40$ pF ($40 = 39 + 1$).

Results obtained within the nearest-neighbor approximation and those from taking into account the interaction between all the columns compare favorably with the experimental results. The inclusion of all the mutual inductances between the columns only (Eq. [19]) agrees

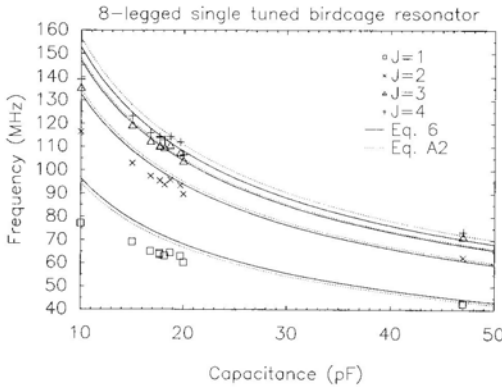


FIG. 6. The frequency dependence of the resonant modes of an eight-column single-tuned resonator, measured and calculated from Eq. [6] (without the ring mutual inductances) and from Eq. [A.2] (including all the mutual inductances).

Table 2
Measured and Calculated Capacitance Values for Eight-Legged Double-Tuned Birdcage Resonator

	C_{odd} (pF)	C_{even} (pF)
Experimental	526	40.0
Calculated		
No mutual inductance	463	30.5
Nearest-neighbor columnar mutual inductance included	454	39.9
All columnar mutual inductances included	454	39.3
Nearest-neighbor columnar and ring mutual inductances included	512	39.6
All mutual inductances included	522	39.4

with the experimental values within 14% (C_{odd}) and 2% (C_{even}). Further inclusion of the mutual inductances between the ring segments reduces the discrepancy to less than 1% for $C = 526$ pF and 2% for $C = 40$ pF.

In this work, we did not investigate the RF efficiency of this type of coil. To compare the theory that predicts the values of the capacitors and the experiment, we only used fixed capacitors. Therefore, our coils are not finely tuned and finely matched. Any RF efficiency measurements requires complete tuning and matching as well as experimentation with lossy samples. Here, we simply tried to show the principle of double tuning by building prototype coils and proving that the theory and the experiment are in good agreement.

CONCLUSIONS

A theoretical approach to design birdcage resonators was presented. The resonant frequencies of a symmetrical birdcage calculated using all mutual inductances the columns and ring segments agree well with experimental values. By allowing the capacitances in the columns to be distributed unequally but periodically, it is possible to tune the birdcage to multiple frequencies. Closed-form expressions for the two capacitances necessary to double tune a resonator to two given frequencies were given in terms of the frequencies and the self- and mutual inductances. Calculated and measured values of the capacitances of a birdcage double-tuned to proton and carbon agree to within 1% and 2%, respectively.

APPENDIX A

In this appendix, we show how the mutual inductances of the ring segments modify the expressions of the resonant frequencies as well as the two capacitances necessary for double tuning. The calculations are carried out for an eight-column birdcage; configurations with a different number of columns can be treated along the same lines.

The mutual inductance between a ring segment and the one directly under (above) it in the other ring is denoted as m_0 , that between two touching segments of the same ring m_{1T} , and so on. The quantity m_{1B} denotes the mutual inductance between a ring segment in one

ring and a ring segment in the other ring, one section removed.

In our case, the quantities $m_{2T} = m_{2B} = 0$. Notice also that the mutual inductances between the ring segments and the columns are all zero because of the orthogonality of their respective directions. When the capacitances are all equal, the mesh currents I_n are related by an equation similar to Eq. [1], namely

$$\left[\left(2L + 2l - 2M - 2m_0\omega^2 - \frac{2}{C} \right) I_n - [(L - 2M = 2m_{1T} - 2m_{1B}) + M_2]\omega^2 - \frac{1}{C} \{ I_{n-1} + I_{n+1} \} - \omega^2 \{ m - 2M_2 + M_3 \} [I_{n-2} + I_{n+2}] - \omega^2 \{ M_2 - 2M_3 - 2m_{3b} + 2m_{3t}M_4 \} [I_{n-3} + I_{n+3}] - \omega^2 \{ M_3 - 2m_4 - 2m_{4b} + 2m_{4t} + M_5 \} [I_{n-4} + I_{n+4}] = 0 \right. \quad [A1]$$

If the mutual inductances of the ring segments are neglected in the above equation, Eq. [1] results. Using Eq. [5] in Eq. [A.1], the resonant frequency of mode J is given by

$$\omega_J^2 = b_0 \frac{1 - \cos(2\pi J/8)}{1 - \sum_{i=1}^{i=4} (b_0/b_i) \cos(2\pi J/8) i} \quad [A2]$$

where

$$b_0 = \frac{1}{C(L + l - M - m_0)} \quad [A3]$$

$$b_1 = \frac{1}{C(L - 2M + 2m_{1m} - 2m_{1T} + M_2)} \quad [A4]$$

$$b_i = \frac{1}{C(M_{i-1} - 2M_i - 2m_{iB} + 2m_{iT} + M_{i+1})}, \quad i = 2, 3, 4. \quad [A5]$$

Notice the sign change in front of the terms in m_{iT} and m_{iB} for $i \geq 3$ because of the relative directions of the currents in the ring segments, which are two or more sections removed from one another. For other values of N , this sign change occurs when $i > N/4$.

APPENDIX B

The contribution of the mutual inductances of the ring segments to the two capacitances necessary for double tuning is analyzed in this appendix. Again, the results are valid for the case of an eight-column birdcage; larger numbers of columns can be treated similarly. From Kirchoff's law, equations similar to Eqs. [17] and [18], with the terms m_{iT} and m_{iB} included, lead to Eqs. [22] to [24], where the constants b'_{11} and b'_{12} given

below should be used instead of b_{11} and b_{12} :

$$b'_{11} = b_{11} - 2m_0 + 2(m_{4B} - m_{4T}) \cos\left(\frac{2\pi J}{N}\right) \quad [B1]$$

$$b'_{12} = b_{12} + 2(m_{1B} - m_{1T})(1 + e^{j2\pi J/N}) + 2(m_{3T} - m_{3B})(e^{-j2\pi J/N} + e^{j2\pi J/N}) \quad [B2]$$

where b_{11} and b_{12} are given by Eq. [21].

REFERENCES

1. D. L. Rothman, K. L. Behar, H. P. Hetherington, ^1H -observed ^{13}C -decoupled spectroscopic measurements of lactate and glutamate in the rat brain *in vivo*. *Proc. Natl. Acad. Sci. USA* **82**, 911-920 (1985).
2. S. M. Fitzpatrick, H. P. Hetherington, K. L. Behar, R. G. Shulman, The flux from glucose to glutamate in the rat brain *in vivo* as determined by ^1H -observed ^{13}C -edited NMR spectroscopy. *J. Cereb. Blood Flow Metab.* **10**, 170-179 (1990).
3. N. Beckmann, ^{13}C NMR for the assessment of human brain glucose metabolism *in vivo*. *Biochemistry* **30**, 6362-6366 (1991).
4. N. Beckmann, in "NMR, Basic Principles and Progress" (J. Seeling, M. Rudin, Eds.), Vol. 28, p. 73, Springer-Verlag, Berlin, 1992.
5. P. C. M van Zijl, A. S. Chesnick, D. DesPres, C. T. W. Moonen, J. Ruiz-Cabello, P. van Gelderen, *In vivo* proton spectroscopy and spectroscopic imaging of ^{13}C -glucose and its metabolic products. *Magn. Reson. Med.* **30**, 544-551 (1993).
6. P. C. M. van Zijl, P. B. Barker, B. J. Soher, J. Gillen, P. A. Bottomley, J. Duyn, C. T. W. Moonen, R. G. Weiss, Proton spectroscopic imaging of ^{13}C -labeled compounds on a 1.5 Tesla standard clinical imager, in "Proc., SMRM, 12th Annual Meeting, New York, 1993," p. 373.
7. A. M. Uluğ, J. H. Shi, P. B. Barker, P. C. M. van Zijl, Two-port double-tuned volume resonators for proton detected heteronuclear studies on a clinical scanner, in "Proc., SMR, 2nd Annual Meeting, New York, 1994," p. 1120.
8. A. Heerschap, P. R. Luyten, J. I. van der Heyden, L. J. M. P. Oosterwaal, J. A. den Hollander, Broadband proton-decoupled natural abundance ^{13}C NMR spectroscopy of humans at 1.5 T. *Nucl. Magn. Reson. Biomed.* **2**, 1-9, (1989).
9. J. Murphy-Boesch, R. Stoyanova, R. Srinivasan, T. Willard, D. Vigneron, S. Nelson, J. S. Taylor, T. Brown, Proton-decoupled ^{31}P chemical shift imaging of the human brain in normal volunteers. *Nucl. Magn. Reson. Biomed.* **6**, 173-180, (1993).
10. P. R. Luyten, G. Bruntink, F. M. Sloff, J. W. A. H. Vermeulen, J. I. van der Heijden, J. A. den Hollander, A. Heerschap, Broadband proton decoupling in human ^{31}P NMR spectroscopy. *Nucl. Magn. Reson. Biomed.* **1**, 177-183 (1989).
11. C. E. Hayes, W. A. Edelstein, J. F. Schenk, O. M. Mueller, M. Eash, An efficient, highly homogeneous radiofrequency coil for whole-body NMR imaging at 1.5 T. *J. Magn. Reson.* **63**, 622-628 (1985).
12. H. Breuer, Small NMR probe for use in homogeneous fields. *Rev. Sci. Instrum.* **36**, 1666-1669 (1965).
13. C. N. Chen, D. I. Hoult, V. J. Sank, Quadrature detection coils: a factor $\sqrt{2}$ improvement in sensitivity. *J. Magn. Reson.* **54**, 324 (1983).
14. J. Tropp, The theory of the birdcage resonator. *J. Magn. Reson.* **82**, 51-62 (1989).
15. R. Pascone, T. Vullo, J. Farrelly, P. T. Cahill, Explicit treatment of mutual inductance in eight-column birdcage resonators. *Magn. Reson. Imaging* **10**, 401-410 (1992).
16. T. K. F. Foo, C. E. Hayes, Y.-W. Kang, An analytical model for the design of RF resonators for MR body imaging. *Magn. Reson. Med.* **21**, 165-177 (1991).
17. M. D. Harpen, Equivalent circuit for birdcage resonators. *Magn. Reson. Med.* **29**, 263-268 (1993).
18. M. D. Harpen, Cylindrical coils near self-resonance. *Magn. Reson. Med.* **30**, 489 (1993).
19. A. R. Rath, Design and performance of a double-tuned bird-cage coil. *J. Magn. Reson.* **86**, 488-495 (1990).
20. P. M. Joseph, D. Lu, A technique for double resonant operation of birdcage imaging coils. *IEEE Trans. Med. Imaging* **8**, 286-294 (1989).
21. J. Murphy-Boesch, R. Srinivasan, L. Carvajal, T. R. Brown, Two

- configurations of the four-ring birdcage coil for ^1H imaging and ^1H -decoupled ^{31}P spectroscopy of the human head. *J. Magn. Reson. B* **103**, 103–114 (1994).
22. J. Tropp, N. Sailasuta, J. C. Chen, P. Calderon, R. Hurd, A dual-tuned quadrature volume resonator for proton-decoupled phosphorus spectroscopy of human head at 1.5 T, in "Proc., SMR, 2nd Annual Meeting, New York, 1994," p. 1121.
 23. J. T. Vaughan, H. P. Hetherington, J. W. Pan, P. J. Noa, G. M. Pohost, A high-frequency double-tuned resonator for clinical NMR, in "Proc., SMRM, 12th Annual Meeting, New York, 1993," p. 306.
 24. J. T. Vaughan, H. P. Hetherington, G. M. Pohost, Multiply tuned high frequency volume coils for clinical NMR, in "Proc., SMR, 2nd Annual Meeting, New York, 1994," p. 1119.
 25. T. A. Cross, S. Muller, W. P. Aue, Radiofrequency resonators for high-field imaging and double-resonance spectroscopy. *J. Magn. Reson.* **62**, 87–98 (1985).
 26. N. Ashcroft, D. Mermin, "Solid State Physics," Saunders, Orlando, 1976.
 27. J. S. Blakemore, "Solid State Physics," 3rd ed., Saunders, London, 1974.
 28. C. Kittel, "Introduction to Solid State Physics," 6th ed., Wiley, New York, 1986.
 29. J. M. Ziman, "Principles of the Theory of Solids," Cambridge Press, New York, 1972.
 30. L. Nolinger, M. C. Prammer, J. S. Leigh, Jr., A multiple-frequency coil with a highly uniform B_1 field. *J. Magn. Reson.* **81**, 162–166 (1988).
 31. F. W. Grover, "Inductance Calculations," D. Van Nostrand, New York, 1946.